# Machine learning-assisted screening of small-molecule drugs for suppressing protein aggregation and ROS generation based on ECL and CV dual-mode signals amplified by DNA

Jiaqi Shi,[a] Wenxiu Zhu,[a] Jingyu Yan,[a] Cong Xiao,[a] Huiqin Yao,[b] Lingchen Meng,[b] Hongyun Liu,[a,*] Lanqun Mao[a,*]

[a] Key Laboratory of Radiopharmaceuticals, Ministry of Education, College of Chemistry, Beijing Normal University, Beijing 100875, Peoples' Republic of China.

[b] School of Public Health, Key Laboratory of Environmental Factors and Chronic Disease Control, Ningxia Medical University, Yinchuan 750004, People's Republic of China.

* Corresponding author: liuhongyun@bnu.edu.cn (H.L.); lqmao@bnu.edu.cn. (L.M.).

# Contents

**Experimental Section** ..... **S3**

**Experimental Reagents** ..... **S3**

**Instrumentation and Characterization** ..... **S4**

**Characterization of MUA/MCH Self-Assembly Membranes (SAMs)** ..... **S5**

**Preparation of α-Syn Monomers** ..... **S5**

**TEM Characterization of Protein Aggregation** ..... **S6**

**Construction of the mCherry-α-Syn Cell Line** ..... **S6**

**Induction of Intracellular α-Syn Aggregates** ..... **S7**

**Fluorescence Microscopy Imaging and Quantitative Analysis** ..... **S7**

**Image Processing** ..... **S7**

**Cytotoxicity Assay** ..... **S7**

**ROS Measurement** ..... **S7**

**Results and Discussion** ..... **S8**

**Figure S1.** ..... **S8**

**Figure S2.** ..... **S9**

**Figure S3.** ..... **S10**

**Figure S4.** ..... **S11**

**Figure S5.** ..... **S12**

**Figure S6.** ..... **S12**

**Figure S7.** ..... **S13**

**Table S1.** ..... **S14**

**Table S2.** ..... **S15**

**Figure S8.** ..... **S15**

**Monitoring ROS Generation by UV** ..... **S15**

**Figure S9.** ..... **S16**

**Preparing mCherry-α-Syn** ..... **S17**

**Figure S10.** ..... **S18**

**Figure S11.** ..... **S19**

**References** ..... **S19**

## Experimental Section

### Reagents

α-Synuclein 31-54 (α-Syn) was purchased from Nanjing Peptide Biotechnology Co., Ltd., with a purity > 95%. HeLa cells were obtained from Invitrogen (USA). The plasmid DNA (pLV2-CMV-mCherry-SNCA(human)-Puro) was sourced from the Miaoling Plasmid Platform (Wuhan), and the transfection reagent M5 Hiper Lipo 2000 was purchased from Mei5 Biotechnology Co., Ltd. (Beijing). All reagents were of analytical grade and were used without further purification. Deoxyribonucleic acid sodium salt (DNA) from salmon, glutathione (GSH), cysteine (Cys), 1,1,1,3,3,3-hexafluoro-2-propanol (HFIP), catalase, Tris(2,2′-bipyridyl)dichlororuthenium(II) hexahydrate ($Ru(bpy)_3Cl_2$), 4-(2-hydroxyethyl)piperazine-1-ethanesulfonic acid (HEPES), 2',7'-dichlorodihydrofluorescein diacetate (DCFH-DA), 3-(4,5-dimethyl-2-thiazolyl)-2,5-diphenyl-2H-tetrazolium bromide (MTT), and dimethyl sulfoxide (DMSO) were purchased from Sigma–Aldrich (Shanghai). Ascorbic acid (AA), *N*-(3-dimethylaminopropyl)-*N*'-ethylcarbodiimide hydrochloride (EDC) and *N*-hydroxysuccinimide (NHS) were purchased from Innochem (Beijing). $K_3Fe(CN)_6$, 11-mercaptoundecanoic acid (MUA), 6-mercapto-1-hexanol (MCH), ethanolamine (EA), testesα-ketoglutaric acid (α-KG), chloroquine (CQ), epinephrine (EPI), dopamine (DA), ethylenediaminetetraacetic acid disodium salt (EDTA), pyrroloquinoline quinone (PQQ), *N*,*N*,*N*',*N*'-tetramethyl-p-phenylenediamine dihydrochloride (TMPD), vitamin D (VD), isopropyl alcohol (IPA), edaravone (1-pheny-3-methyl-5-pyrazolone, PMP) and phosphotungstic acid were purchased from Aladdin Chemical Co. Ltd. (Shanghai). Diethylenetriaminepentaacetic dianhydride (DTPA), 1,2-dimethyl-3-hydroxy-4-pyridinone (deferiprone), and cell culture reagents, including Dulbecco's modified Eagle’s medium (DMEM), fetal bovine serum (FBS), penicillin–streptomycin (dual

antibiotics), and trypsin solution, were purchased from Macklin Biochemical Co., Ltd. (Shanghai). Deionized water was obtained from a Millipore purification system (18.2 MΩ cm). All the experiments were conducted at room temperature (~25 °C) under standard atmospheric conditions unless otherwise specified.

**Instrumentation and Characterization**

Electrochemiluminescence (ECL) and cyclic voltammetry (CV) measurements were simultaneously carried out on an MPI-E electrochemical workstation (Xi'an Remex Electronics Technology Co., Ltd., China) by using a conventional three-electrode system: a modified gold electrode as the working electrode, a platinum electrode as the counter electrode, and an Ag/AgCl electrode (saturated KCl) as the reference electrode. During detection, the voltage of the photomultiplier tube (PMT) was set to 600 V. ECL and CV measurements were usually performed in a pH 7.4 HEPES buffer (20 mM) solution containing 0.8 mM $Ru(bpy)_3^{2+}$ and 0.3 mg·mL$^{-1}$ DNA, unless otherwise specified. Electrochemical impedance spectroscopy (EIS) was conducted on a CHI 660E electrochemical workstation (Shanghai CH Instruments Co., Ltd.) using a three-electrode system: a modified Au electrode as the working electrode, a saturated calomel electrode (SCE) as the reference electrode, and a platinum electrode as the counter electrode. To obtain stable and reproducible signals, the ECL and CV results were taken from the second cycle of the test. EIS was tested in 1.0 mM $Fe(CN)_6^{3-/4-}$ (containing 1.0 M NaCl) from 0.1~$10^5$ Hz with a 5 mV amplitude at 0.17 V (vs. SCE). The obtained EIS data were fitted by ZsimpWin software` with the Randles equivalent circuit model.

Ultraviolet (UV) absorption spectra were recorded on a UV-2600 spectrometer (Shimadzu, Japan). Transmission electron microscopy (TEM) was performed on a Talos F200S transmission electron microscope (Thermo Fisher Scientific, USA). X-ray

photoelectron spectroscopy (XPS) was performed on an ESCALAB 250Xi X-ray spectrometer (Thermo Fisher Scientific, USA). The XPS samples were prepared on the surface of quartz prepared in the same way as the gold electrode. Atomic force microscopy (AFM) measurements were performed using a Bruker Dimension Icon microscope (Germany). The AFM samples were prepared on gold-coated silicon wafers using the same modification procedure as that applied to the gold electrode. The cytotoxicity assay was performed using a Synergy H1 microplate reader (BioTek, USA) to measure the absorbance at 570 nm and thus calculate cell viability. Confocal images were acquired using an FV1000-IX81 laser scanning confocal microscope (Olympus, Japan).

**Characterization of MUA/MCH Self-Assembly Membranes (SAMs)**

The apparent coverage ($\theta$) of MUA/MCH on the electrode surface could be estimated through EIS results by: $\theta = 1 - \frac{R_{CT}^0}{R_{CT}}$,[1,2] where $R_{CT}^0$ is the charge-transfer resistance ($R_{CT}$) value of bare Au electrode and $R_{CT}$ is the $R_{CT}$ value of the monolayer-covered (i.e. MUA/MCH-covered) electrode, respectively. According to the results in Figure 1A, $\theta$ was estimated to be 0.93 ± 0.04 with $R_{CT}^0$ = 91 ± 52 Ω, and $R_{CT}$ = 1250 ± 110 Ω. It was demonstrated that MUA/MCH formed a near-monolayer coverage on the Au electrode surface and the surface coverage of carboxyl groups was sufficiently high to further immobilize proteins. Furthermore, based on the molecular chain length of MUA (1.7 nm),[3] the maximum apparent thickness of MUA/MCH mixed SAMs was estimated to be about 1.7 nm, indicating that MUA/MCH modification would not impede electron transfer between the electrochemical probes and the electrode surface.

**Preparation of α-Syn Monomers**

α-Syn powder was dissolved in HFIP at a concentration of 1 mg·mL$^{-1}$. The

solution was vortexed until completely dissolved and then placed in a 4 °C refrigerator overnight to remove α-Syn preaggregates.[4] The solution was then divided into aliquots as needed, and the solvent was dried under a gentle stream of nitrogen to obtain a transparent α-Syn film in the aliquot tube. The tubes were sealed and stored at –20 °C until use.

**Transmission Electron Microscopy (TEM) Characterization of Protein Aggregation**

TEM samples were prepared according to a previously reported method.[5] A 25 μM α-Syn or other required solution was incubated with either buffer or an equivalent amount of Cu(II) at 37 °C with continuous stirring for 24 h. Then, 10 μL of the sample solution was dropped onto a copper grid and allowed to adsorb for 5 min. After the excess solution was removed with filter paper, the copper grid was washed three times with deionized water and stained with a 2% phosphotungstic acid solution for 2 min. The excess solution was removed, and the grid was left to dry prior to examination.

**Construction of the mCherry-α-Syn Cell Line**

To establish a cell model for dynamically monitoring α-Syn aggregation, the pLV2-CMV-mCherry-SNCA (human)-Puro plasmid was transiently transfected into HeLa cells using the Lipo 2000-mediated lipofection method.[6] Specifically, 10 μL of large-scale extracted plasmid solution (~2 $\mu g \cdot \mu L^{-1}$) was mixed with 48 μL of Lipo2000 transfection reagent and incubated for 15 min. Then, 10 mL of serum-free and antibiotic-free high-glucose DMEM was added and mixed thoroughly. The original medium in the cell culture dish was replaced with this mixture, and the cells were incubated at 37 °C in a 5% $CO_2$ incubator for 6 h before being switched to complete medium. After 24 h of transfection, the distribution of red fluorescence was preliminarily observed using a confocal fluorescence microscope. Successful

transfection was confirmed by the presence of uniform mCherry-specific red fluorescence signals (excitation wavelength: 587 nm, emission wavelength: 610 nm[7]) in the cytoplasm of the transfected cells. The fluorescence of the mCherry-α-Syn cell line obtained by this method was maintained for 3–5 days.

**Induction of Intracellular α-Syn Aggregates**

In accordance with methods described in the literature,[8] complete medium containing 15 μM Cu(II) (prepared by adding 1 mM $CuCl_2$ in PBS) was used to treat the transfected mCherry-α-Syn cells for 24 h, followed by observation under a confocal microscope.

**Fluorescence Microscopy Imaging and Quantitative Analysis**

Confocal microscopy was performed with an excitation wavelength of 587 nm and an emission wavelength of 610 nm. For each experimental group, 3 random fields of view were selected, and 1–2 cells per field were analyzed.

**Image Processing**

Using ImageJ (NIH), aggregates were defined as regions with a fluorescence intensity ≥ 3 times the cytoplasmic background (ROI analysis). The "Analyze Particles" function was employed to automatically count the area of bright mCherry-α-Syn aggregate spots per cell.

**Cytotoxicity Assay**

An MTT assay was subsequently performed. MTT solution was added to the cell culture medium at a final concentration of 0.5 $mg \cdot mL^{-1}$. After 4 h of incubation, the medium was removed, and DMSO was added to dissolve the formazan crystals. Once fully dissolved, the absorbance at 570 nm was measured using a microplate reader (BioTek Synergy H1), and the cell viability was calculated (with the untreated group set to 100%).

### ROS Measurement

The intracellular ROS levels were detected using the fluorescent probe DCFH-DA. Upon entering cells, this probe is oxidized by ROS to produce the fluorescent compound 2',7'-dichlorofluorescein (DCF). Transfected mCherry-α-Syn cells were seeded into confocal dishes or 96-well plates. After cell attachment, the medium was replaced with complete medium containing 15 μM Cu(II) or complete medium containing 15 μM Cu(II) and 15 μM of the corresponding small-molecule drug. After 4 h of incubation at 37 °C, the medium was replaced with complete medium containing 10 μM DCFH-DA, and the mixture was incubated for an additional 30 min at 37 °C. The medium was subsequently discarded, and the cells were washed 3 times with DPBS buffer. DCF fluorescence emission at 525 nm was observed under a confocal microscope at an excitation wavelength of 488 nm.

## Results and Discussion

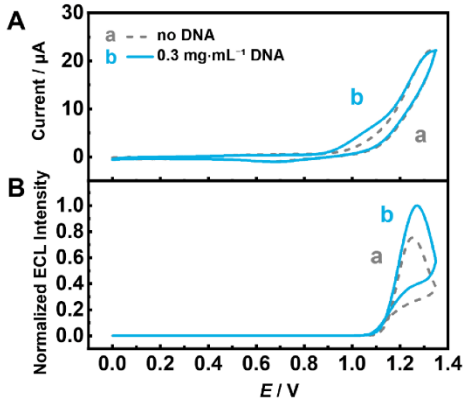


$$Ru(bpy)_3^{2+} \rightleftharpoons Ru(bpy)_3^{3+} + e^- \quad (1)$$

$$Ru(bpy)_3^{2+} + e^- \rightleftharpoons Ru(bpy)_3^{+} \quad (2)$$

$$Ru(bpy)_3^{3+} + Ru(bpy)_3^{+} \rightarrow Ru(bpy)_3^{2+*} + Ru(bpy)_3^{2+} \quad (3)$$

$$Ru(bpy)_3^{2+*} \rightarrow Ru(bpy)_3^{2+} + h\nu\ (610\ nm) \quad (4)$$

$$Ru(bpy)_3^{3+} + DNA\text{–}G \rightarrow Ru(bpy)_3^{2+} + DNA\text{–}G_{Ox} \quad (5)$$

$$Ru(bpy)_3^{3+} + DNA\text{–}G_{Ox} \rightarrow Ru(bpy)_3^{2+*} + DNA\text{–}G_{2Ox} \quad (6)$$

**Figure S1.** (A) CV and (B) ECL curves for α-Syn-modified electrodes (a) without and (b) with 0.3 mg·mL$^{-1}$ DNA in 0.8 mM $Ru(bpy)_3^{2+}$ in pH 7.4 buffers at a scan rate of 0.05 V·s$^{-1}$. (C) The CV and ECL mechanism of $Ru(bpy)_3^{2+}$ without (1~4) and with DNA (1, 4~6).[9]

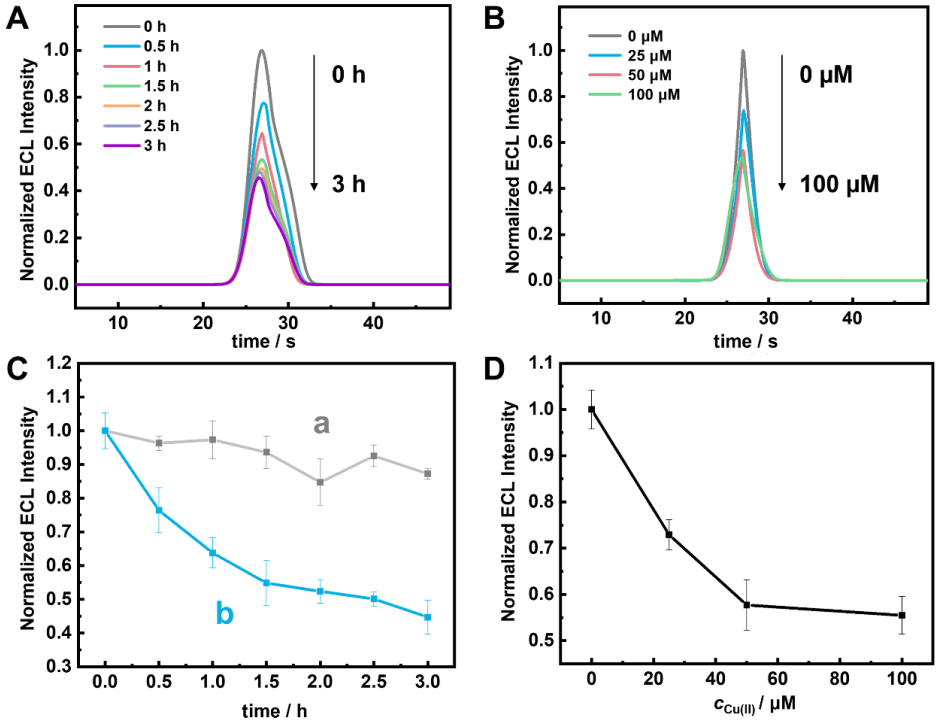


**Figure S2.** ECL results of the α-Syn-modified electrode in 0.8 mM $Ru(bpy)_3^{2+}$ with 0.3 mg·mL$^{-1}$ DNA in pH 7.4 buffer at a scan rate of 0.05 V·s$^{-1}$ in response to (A) incubation time with 50 μM Cu(II) and (B) concentration of copper ($c_{Cu(II)}$) for 2 h. Normalized ECL intensity of α-Syn-modified electrodes (C) with incubation time in (a) buffer and (b) 50 μM Cu(II) solution and (D) with $c_{Cu(II)}$ after incubation for 2 h.

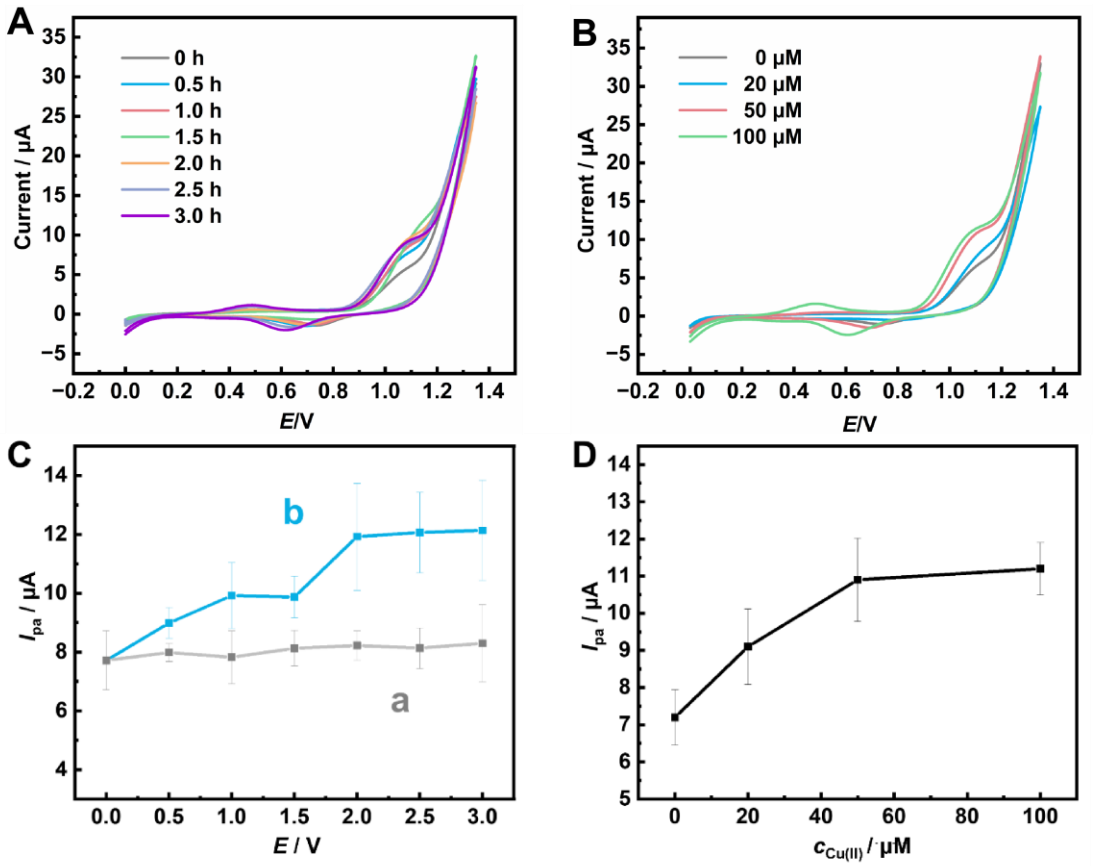


**Figure S3.** CV responses of the α-Syn-modified electrode in 0.8 mM $Ru(bpy)_3^{2+}$ with 0.3 mg·mL$^{-1}$ DNA in pH 7.4 buffers at a scan rate of 0.05 V·s$^{-1}$ after incubation with (A) 50 μM Cu(II) and (B) concentrations of copper ($c_{Cu(II)}$) for 2 h. $I_{pa}$ of α-Syn-modified electrodes (C) with incubation time in (a) buffer and (b) 50 μM Cu(II) solution and (D) with different $c_{Cu(II)}$ concentrations after incubation for 2 h.

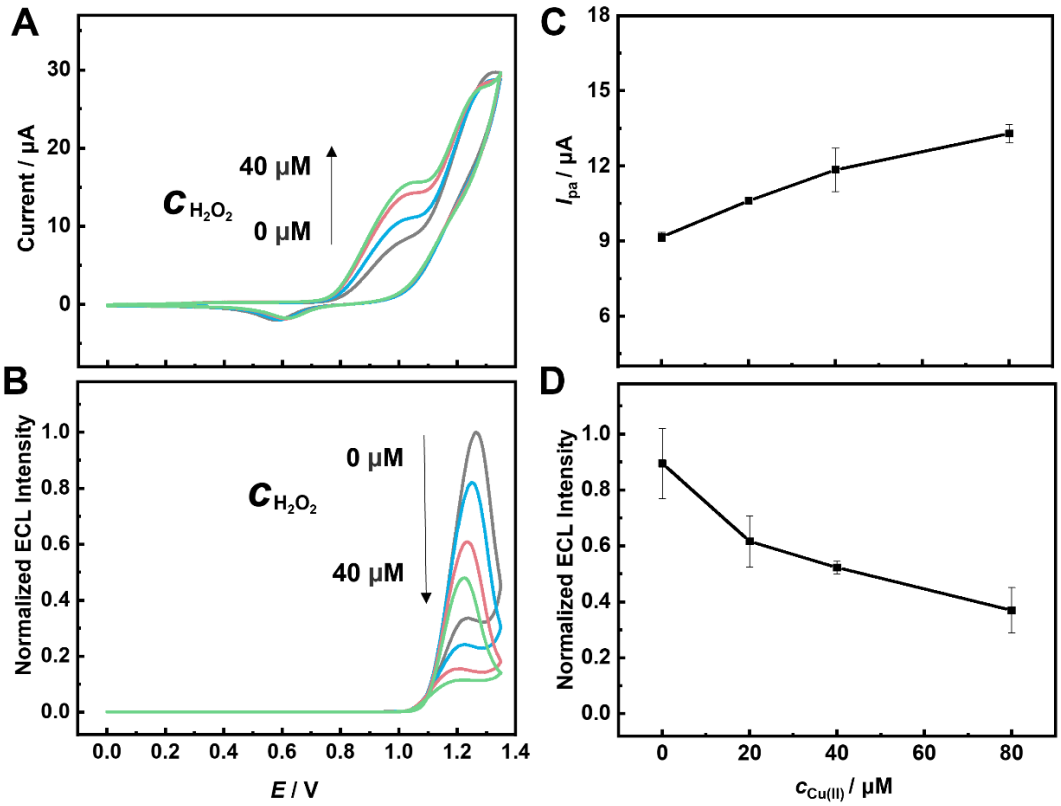


**Figure S4.** Simultaneous (A) CV and (B) ECL response curves of α-Syn-modified electrodes in an electrolyte containing different concentrations of $H_2O_2$, 0.8 mM $Ru(bpy)_3^{2+}$ and 0.3 mg·mL$^{-1}$ of DNA. (C) $I_{pa}$ of CV at 1.05 V and (D) changes in the ECL intensity with different $H_2O_2$ concentrations ($c_{H_2O_2}$). The error bars represent the standard deviation of the experimental results ($n$ = 3).

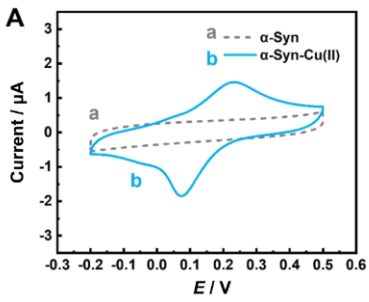


C

| System | $E_0$/V (vs. SCE) | Ref. |
|---|---|---|
| $O_2/H_2O_2$ | 0.06 | 10 |
| α-Syn-Cu(II)/α-Syn-Cu(I) on electrode surface in aqueous dispersion | 0.04 | This work |
| | −0.02 | 10 |
| Cytochrome *c* | 0.01 | 11 |
| Ascorbic Acid | −0.19 | 10 |
| Cytochrome *b* | −0.20 | 11 |
| Glutathione | −0.47 | 10 |
| Vitamin $B_{12}$ | −0.48 | 10 |

**Figure S5.** CVs for α-Syn-modified electrodes at 0.1 $V \cdot s^{-1}$ in (A) air-equilibrated pH 7.4 buffer (a) before and (b) after incubation Cu(II), and (B) α-Syn-Cu(II) modified electrodes in (a) $N_2$- and (b) $O_2$-purged pH 7.4 buffer solution, respectively. (C) Comparison of conditional redox potentials ($E^{0'}$) between α-Syn-Cu(II) and intracellular/extracellular electroactive species and antioxidants.[10,11]

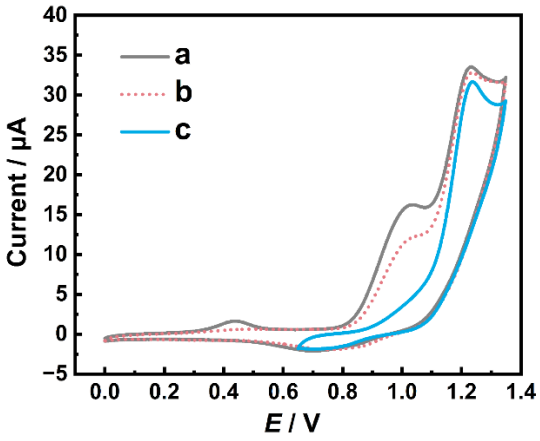


**Figure S6.** CV results of the α-Syn-Cu(II) modified electrode in 0.8 mM $Ru(bpy)_3^{2+}$ with 0.3 $mg \cdot mL^{-1}$ DNA in pH 7.4 buffers at a scan rate of 0.05 $V \cdot s^{-1}$. The response scan range was set for (a) the 1st and (b) the 3rd cycle from 0 to 1.35 V, and (c) for the 1st cycle from 0.65 to 1.35 V, respectively.

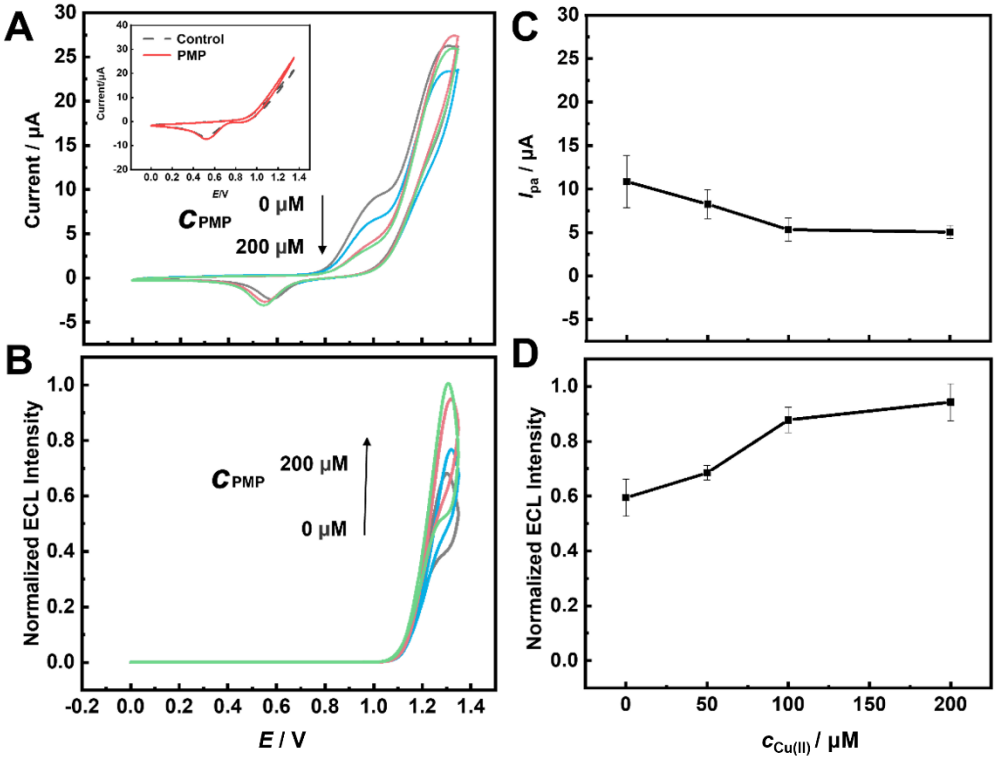


**Figure S7.** Simultaneous (A) CV and (B) ECL response curves of α-Syn-modified electrodes in an underlying solution containing different concentrations of PMP ($c_{PMP}$), 0.8 mM $Ru(bpy)_3^{2+}$, 0.3 mg·mL$^{-1}$ DNA and 40 μM $H_2O_2$. Lines represent $c_{PMP}$ = 0, 0.05, 0.1 and 0.2 mM. (C) $I_{pa}$ of CVs at 1.05 V and (D) ECL intensity of $c_{PMP}$. Inset A: CV curves of 0.1 mM PMP in buffer, showing no electrochemical activity within the tested potential range and no formation of interfering species. The error bars represent the standard deviation of the experimental results ($n$ = 3).

**Table S1.** Molecular structures of potential small-molecule drugs

| Small Molecules | Structure |
|---|---|
| **DA**<br>(Dopamine) | 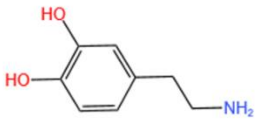 |
| **EPI**<br>(Epinephrine) | 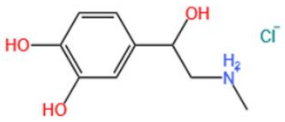 |
| **α-KG**<br>(α-Ketoglutaric acid) | 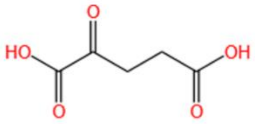 |
| **TMPD**<br>(N,N,N′,N′-Tetramethyl-p-phenylenediamine dihydrochloride) | 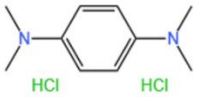 |
| **PQQ**<br>**(**Pyrroloquinoline quinone**)** | 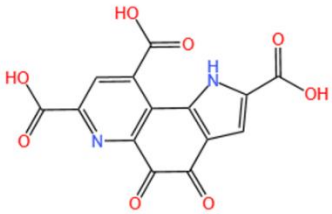 |
| **CQ**<br>(Clioquinol) | 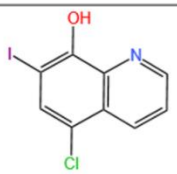 |
| **GSH**<br>(Glutathione) | 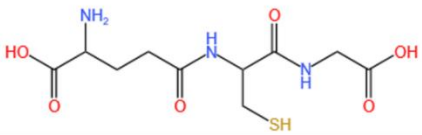 |
| **Cys**<br>(Cysteine) | 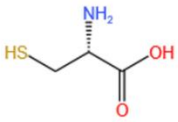 |
| **EDTA**<br>(Ethylenediaminetetraacetic acid tetrasodium salt hydrate) | 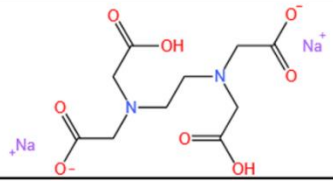 |

**Table S2.** LDA results and correlation formulas for discrimination

| LDA | | Factor 1 | Factor 2 |
|---|---|---|---|
| Proportion | | 76.41% | 23.59% |
| Coefficients | $E'$ | 3.500 | 0.348 |
| | $I'_{pa}$ | -0.127 | -2.079 |
| Correlation formulas | | $[E']$*3.500 - $[I'_{pa}]$*0.127 | $[E']$*0.348 - $[I'_{pa}]$*2.079 |

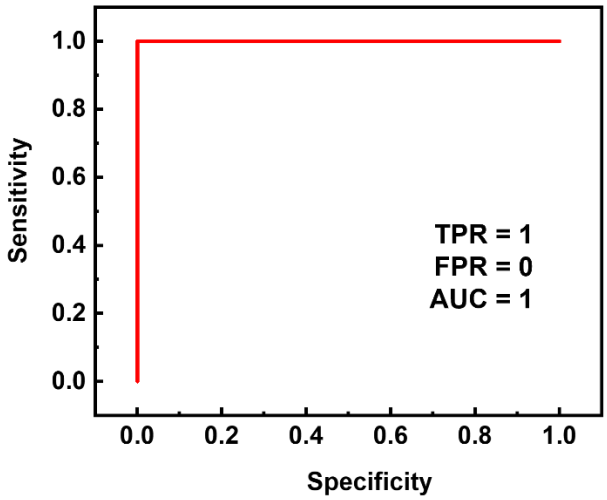


**Figure S8**. ROC curve, TPR, and FPR analyses revealed that the drug screening model can differentiate small-molecule drugs with varying pharmacological effects with high accuracy (AUC = 1).

## Monitoring ROS Generation by UV

The production and scavenging of ROS could be monitored by measuring the absorption peak of AA at 265 nm ($A_{265}$) using UV spectroscopy. In the absence of any potential drug, the $A_{265}$ of the AA solution incubated with the α-Syn–Cu(II)-modified electrodes was significantly lower than that of the AA solution incubated with the α-

Syn-modified electrodes (Figure S9A), indicating that AA consumption was attributable to the generation of ROS induced by Cu(II).

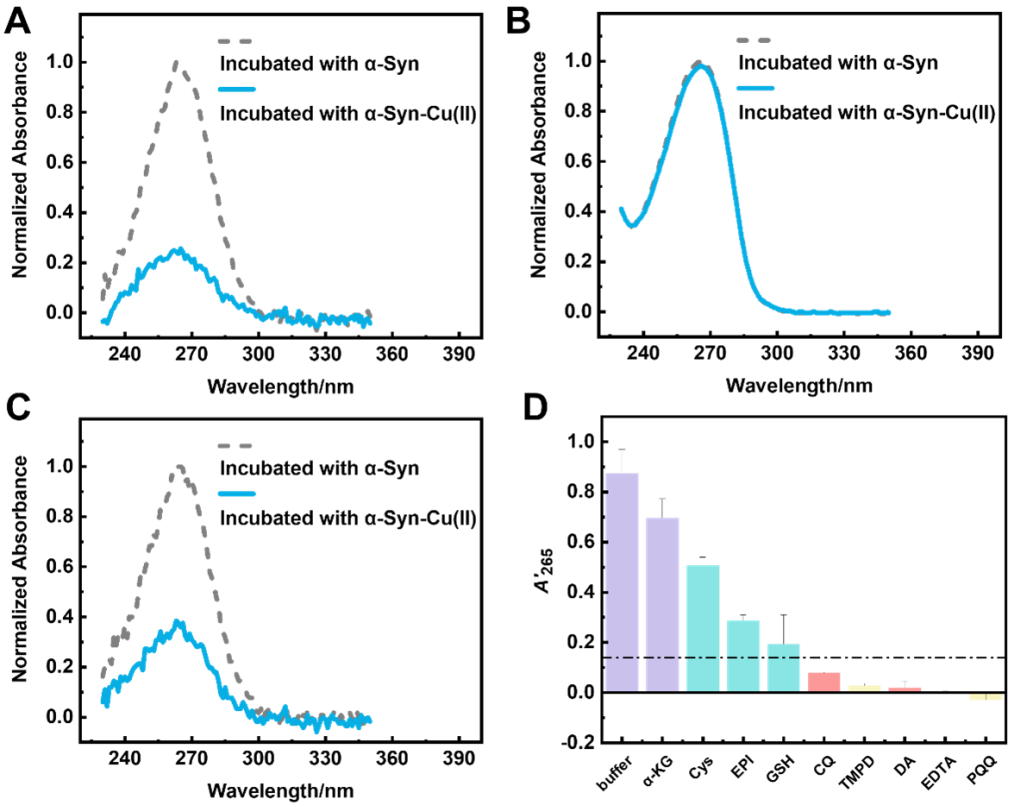


**Figure S9.** UV spectra of (A) 100 μM AA, (B) 100 μM AA + 50 μM DA and (C) 100 μM AA + 50 μM α-KG after incubation with α-Syn- and α-Syn–Cu(II)-modified electrodes for 0.5 h. (D) Comparison of the $A'_{265}$ of 100 μM AA solutions with different drugs with a threshold of 0.1. The error bars represent the standard deviation of the experimental results ($n$ = 3).

When DA was present, the $A_{265}$ values of the solutions incubated with either the α-Syn-Cu(II) or the α-Syn-modified electrodes were nearly identical (Figure S9B). These findings demonstrated that DA inhibited the α-Syn–Cu(II)-catalyzed ROS generation process, suggesting its potential effects on the generation of ROS in biological systems.

In contrast, α-KG, which was previously found to lack the ability to mitigate ROS generation activity, failed to inhibit ROS generation (Figure S9C).

Therefore, we utilized the absorbance reduction ratio ($A'_{265}$) of the AA solution after incubation with the α-Syn- and α-Syn–Cu(II)-modified electrodes to evaluate drug efficacy in terms of ROS inhibition, which was defined as $(A_{265}^0 - A_{265}^1)/A_{265}^0$. Here, $A_{265}^0$ and $A_{265}^1$ represent $A_{265}$ after 0.5 h of incubation of the AA solution with α-Syn- and α-Syn–Cu(II)-modified electrodes, respectively, in the presence of drugs (Figure S9D). A lower $A'_{265}$ value indicates more pronounced ROS-inhibiting efficacy.

As shown in Figure S9D, when $A'_{265} = 0.1$ was used as the threshold to distinguish between effective and ineffective ROS-scavenging drugs, α-KG, Cys, EPI, and GSH were identified as molecules without ROS-scavenging ability, whereas CQ, TMPD, DA, EDTA, and PQQ exhibited ROS-scavenging ability. These results are consistent with the LDA classification results (Figure 5C).

**Preparing mCherry-α-Syn**

The constructed recombinant plasmid was transfected into HeLa cells using the transient transfection method. The positively charged transfection reagent (Lipo 2000) and the negatively charged plasmid formed a complex through electrostatic interactions. The complex entered the cells via endocytosis across the cell membrane, after which the plasmid was released intracellularly and expressed the target gene encoding α-synuclein (α-Syn), enabling the HeLa cells to produce the red fluorescent fusion protein (mCherry). Using confocal microscopy, uniformly dispersed red fluorescence was observed in some HeLa cells within the field of view under 587 nm excitation light (Figure S10), confirming the successful construction of the mCherry-α-Syn cell line.

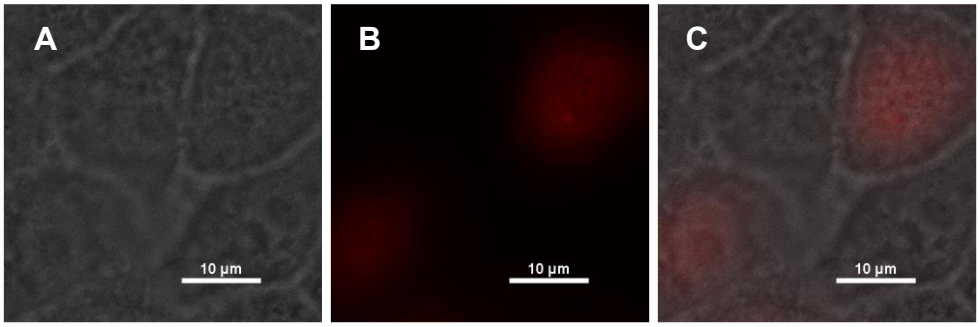


**Figure S10.** (A) Bright-field, (B) 587 nm-excited fluorescence (mCherry), and (C) merged confocal images of mCherry-α-Syn expression in live HeLa cells.

After confirming the successful construction of the mCherry-α-Syn cell line, we simulated the aggregation of α-Syn in vitro. Since Cu(II) can induce significant α-Syn aggregation in cells under similar conditions,[8] to maintain consistency with the experimental conditions, we continued using Cu(II) as the aggregation-inducing factor.

The transfected HeLa cells expressing mCherry-α-Syn were treated with complete medium containing 15 μM Cu(II) for different durations (0, 12, 24, and 36 h). In the absence of Cu(II) (0 h), the red fluorescence was uniformly distributed in both the control and experimental groups. After 12 h of Cu(II) treatment, bright fluorescent puncta began to appear in the treated cells. By 24 h, the number and total area of these aggregates further increased. However, extending the incubation time to 36 h resulted in only a marginal increase in puncta formation (Figure S11).

On the basis of these observations, we speculated that prolonged incubation with Cu(II) induced the formation of mCherry-α-Syn–Cu(II) aggregates. Therefore, we set the duration of Cu(II) treatment for intracellular mCherry-α-Syn aggregation to 24 h for subsequent experiments.

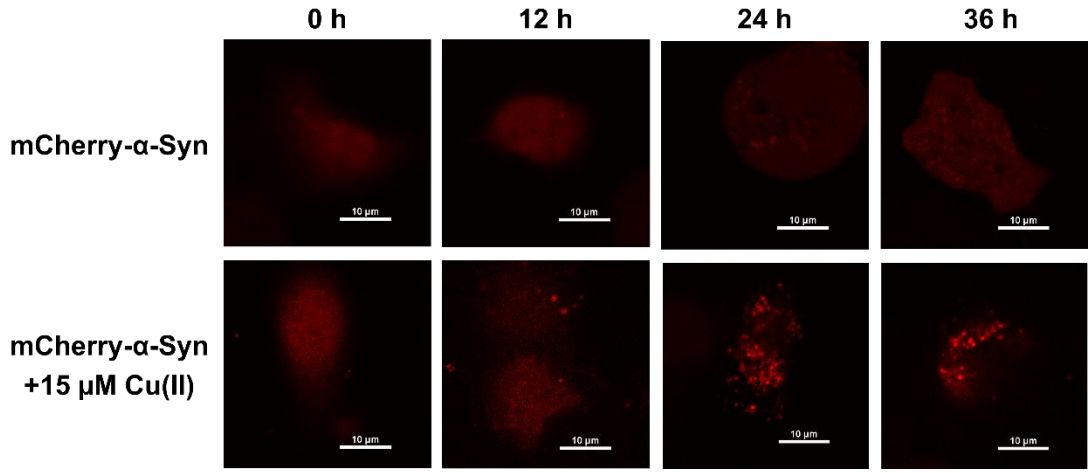


**Figure S11.** Time-dependent mCherry-α-Syn aggregation in cells induced by Cu(II). Cu(II) treatment triggered the formation of high-fluorescence puncta (mCherry-α-Syn–Cu(II)). The results were consistent across 3 independent replicates.

## References

1 H. Han, N. B. Sabani, K. Nobusawa, F. Takei, K. Nakatani and I. Yamashita, *Anal. Chem.*, 2023, **95**, 9729–9733.

2 R. K. Mendes, R. S. Freire, C. P. Fonseca, S. Neves and L. T. Kubota, *J. Braz. Chem. Soc.*, 2004, **15**, 849–855.

3 J. Tong, M. Xiao, K. Wang, Z. Zhao, Y. Chen, Y. Liu, T. Qing, X. Liu and Z. Zhang *ACS Nano*, 2025, **19**, 11358−11370.

4 C. E. MacPhee and C. M. Dobson, *J. Mol. Biol.,* 2000, **297**, 1203–1215.

5 N. Xiong, Y. Zhao, X. Dong, J. Zheng and Y. Sun, *Small,* 2017, **13**, 1601666.

6 P. Yu, R. Wu, S. Cao, Y. Wen, X. Huang, S. Zhao, Y. Lang, Q. Zhao, J. Lin, S. Du, S. Yu and Q. Yan, *Front Microbiol.,* 2023, **14**, 1087484.

7 Z. Li, Q. Wang, Y. Xia, L. Xun and H. Liu, *Antioxidan*ts, 2020, **9**, 985.

8 S. Ray, N. Singh, R. Kumar, K. Patel, S. Pandey, D. Datta, J. Mahato, R. Panigrahi, A. Navalkar, S. Mehra, L. Gadhe, D. Chatterjee, A. S. Sawner, S. Maiti, S. Bhatia, J. A. Gerez, A. Chowdhury, A. Kumar, R. Padinhateeri, R. Riek, G. Krishnamoorthy and S. K. Maji, *Nat. Chem.,* 2020, **12**, 705–716.

9 S. Liu, M. Li, X. Yu, C.-Z. Li and H. Liu, *Chem. Commun.*, 2015, **51**, 13185–13188.

10 C. Wang, L. Liu, L. Zhang, Y. Peng and F. Zhou, *Biochemistry*, 2010, **49**, 8134–8142.

11 D. Jiang, L. Men, J. Wang, Y. Zhang, S. Chickenyen, Y. Wang and F. Zhou, *Biochemistry*, 2007, **46**, 9270–9282.